Benefits and Drawbacks of Hydrogen and Hybrid Multicopter UAVs for Urban Air Mobility

Fontenla-Carrera G.[1], Veiga-López F.[1], Aldao E.[1] and González-Jorge H.[1]

[1]Aerolab, Instituto de Física e Ciencias Aeroespaciais (IFCAE), Universidade de Vigo,
Campus de As Lagoas, Ourense, E-32004, Spain
gabriel.fontenla@uvigo.gal

Abstract

Multicopter Unmanned Aerial Vehicles (UAVs) require less maintenance, are lightweight, exhibit high redundancy in their systems, and their control is simple, making them more agile and precise than other Vertical Take-Off and Landing (VTOL) options. The main problem they present is their shorter flight time, which is limited by the low energy density of batteries and the lack of fixed lifting surfaces. To overcome this drawback, hydrogen is posited as a potential alternative, since fuel cells enable the efficient storage of a greater amount of energy than batteries. In this study, a comparison and analysis of three multicopter models of very different sizes and weights, first powered by batteries and later with hydrogen fuel cells, is carried out. Results show that fuel cells improve range and endurance from 2 to 6 times, but they may limit payload capacity and the ability of the aircraft to operate during energy-demanding maneuvers. Therefore, the possibility of aiming for hybrid technologies (batteries for power demanding and fuel cells for long-range operations) is discussed regarding on the aircraft characteristics. The main conclusions suggest that fuel cells and hybrid models are a real alternative to batteries for multicopters –size-dependent–, but they are much more sensitive to design parameters, thus it is necessary to find a proper balance between weight, size, aerodynamics, cost and performance.

1 Introduction

Europe aspires to deploy Urban Air Mobility (UAM) in coming years, a new transportation model for goods and people involving the use of UAVs to reduce ground traffic congestion and commute times in urban areas. For this purpose, these aircraft must be based on two fundamental pillars: (i) be electric and (ii) capable of performing vertical takeoffs and landings (eVTOL) [9].

Electric propulsion in UAVs offers numerous advantages over combustion: it is aligned with the EU environmental policies, contributing to achieving a carbon-neutral society; it produces less vibrations, which can negatively affect sensors and payload; it is quieter, reducing noise in cities; it is more energy efficient; and maintenance costs are reduced by having fewer moving parts and working at lower temperatures, among others [1][5][17][28]. The most important electrical systems for UAV propulsion are batteries, hydrogen fuel cells, and solar energy, each with its own advantages and drawbacks [17][27]. Batteries are widely used, especially LiPo and Li-ion, but their energy density is still low, not surpassing 200 Wh/kg, limiting aircraft endurance. In fact, it is reached an asymptotic point where, even if the number of batteries is increased, the energy gained is consumed faster due to the increase in weight of the aircraft without achieving an overall improvement [1]. Additionally, charging periods are still long and support few cycles comparing to other technologies [27]. Regarding fuel cells (FC), the most used in UAVs are the Proton Exchange Membrane Fuel Cells (PEMFC). The main advantages compared to batteries are their higher energy density and faster refueling time. However, they are quite expensive, larger in size, and their power density is lower [17][27]. Finally, solar energy allows for recharging during flight, but it requires large surfaces to accommodate solar panels, which, in turn, significantly increases the weight and cost of the UAV. Moreover, its performance capacity relies on the availability of sunlight [27].

On the other hand, VTOL aircraft enable point-to-point services, taking-off and landing directly at customer locations in small designated spaces known as vertiports, without the need for runways or launchers [6][9] [18][27]. According to the literature, UAVs that are suitable for UAM can be classified as: [6][9]:

1. **Vectored thrust.** Propellers are both for VTOL and horizontal flight, as they can modify the propulsion vector by adjusting their tilt. They also have fixed wings that generate lift during horizontal flight.

2. **Lift + cruise.** They are formed by fixed wings that provide lift during horizontal flight and by two independent propulsion units, one for VTOL tasks, and the other for horizontal displacement.

3. **Wingless or Multicopter.** They are the simplest option. Their propellers are fixed and they produce thrust and lift, as they lack fixed lifting surfaces. Aircraft control is achieved by varying relative speeds between rotors.

Generally, aircraft with fixed lifting surfaces can cover greater distances at higher speeds, being more efficient. Nevertheless, multicopters offer high redundancy, lower weight and maintenance, and simple control, making them more agile and ideal for applications that demand precision and maneuverability [9][27]. Therefore, increasing their flight time is essential to enhance its potential and broaden its applications.

While there are numerous studies and examples of fixed-wing UAVs using solar panels, fuel cells, or hybrid systems to address the low energy density of batteries, this situation becomes more complicated for rotary-wing UAVs [1]. Firstly, solar energy is precluded due to the necessity for large surfaces to accommodate solar panels, resulting in excessive weight and cost increments [17][27]. Secondly, rotary-wing aircraft demand more power and exhibit higher dynamic load profiles, posing challenges for hydrogen fuel cells [1]. Lastly, hybrid systems of fuel cells with batteries entail a substantial weight increase that may lead to a loss of payload capacity and performance, as well as being limited by the recharge rate and the cycle life of batteries [1][27]. However, in recent years, certain cases of rotary-wing UAVs with significant payload capacity powered by fuel cells, such as the DS30 from Doosan Mobility Innovation, the H2QUAD 1000 from EnergyOr, the FCAir 1200 from Ballard or the RACHEL project, have succeeded in considerably increasing endurance compared to battery-powered UAVs with similar characteristics [1].

In this work, three multicopter models of very different sizes and weights (small, medium and large) are considered. The performance of these multicopters is simulated under four different flight regimes: (a) horizontal flight, (b) hovering, (c) vertical flight and (d) 45-degree climbing flight, varying their payload capacity, first being powered by batteries and later by fuel cells. The obtained results are analysed, and the possibility of creating hybrid models (fuel cell + batteries) is discussed, as while hydrogen fuel cells improve range and endurance, they may limit payload capacity or the ability to operate during more power-demanding maneuvers. Moreover, in the medium-sized UAV it is detected a very poor performance compared to the other two. Thus, the design specifications of this UAV are evaluated, discussing the identified factors that may be negatively affecting the performance of this model. Conclusions indicate that hydrogen fuel cells and hybrid models are a viable alternative to batteries for multicopters. They can improve hovering endurance and maximum flight range by more than 2 times, even reaching 6 times in some cases, but a much more refined and detailed design is needed, seeking for a balance between aerodynamics, weight, and performance, as these systems tend to increase the weight and size of the UAV while reducing the available power density.

The remainder of this manuscript is organized as follows: Section 2 introduces the methodology of this article, covering the specifications of the selected multicopters and their electric power systems, besides the flight equations applied in simulations. In Section 3, results are presented and analyzed. Moreover, a redesign of the medium-sized UAV, in addition to hybridization in this model and the large one, is proposed to improve their performance. Finally, Section 4 presents the conclusions.

2   Methodology

2.1   Multicopter Characterization

Three different UAVs have been considered including different sizes, payloads and applications. The first is a 1 kg quadcopter that can carry up to 0.5 kg of payload (intended for the rapid delivery of small goods such as medicines), the second is a 7 kg octocopter with up to 7 kg payload capacity (intended for delivery tasks, similar to those designed by Amazon, DHL or Google [7]), and the third is a large multicopter designed as an air taxi to transport two people, weighing 400 kg empty, with a payload capacity of 200 kg. Most of the data for the small and medium models are obtained from [25], which is based on the 3D Robotics' Iris quadcopter and the Turbo Ace's Infinity 9 octocopter, expanded with the information provided by [29]. The large-sized UAV specifications can be found in [6], representing a VoloCity air taxi. Table 1 summarizes all the data from the 3 models necessary for conducting the simulations. It is assumed uniform inflow in the rotor under optimal hover conditions and therefore

the sectional lift coefficient can be considered constant ($\bar{c}_l = c_l$) [16]. Due to lack of data, for the large UAV this coefficient is estimated according to [5] and [16], whereas internal avionic power consumption P_A values were extrapolated based on [15], where a 12 kg drone (including batteries) designed for delivery consumes 0.1 kW. The N/A values appears because passengers and batteries are within the fuselage of the multicopter and thus, they do not compute.

Term	Small UAV	Medium UAV	Large UAV
Number of Blades per Rotor, N	4	3	2
Blade Chord Length, c [m]	0.0157	0.1	0.1
Blade Lift Coefficient, $\bar{c}_l$	0.271	0.4	0.4
Blade Drag Coefficient, c_d	0.012	0.075	0.015
Number of Rotors, n	4	8	18
Rotor Radius, R [m]	0.127	0.216	1.15
Airframe Mass, m_1 [kg]	1.05	7	400
Battery Mass, m_2 [kg]	1	10	300
Payload Mass, m_3 [kg]	0 to 0.5	0 to 7	0 to 200
UAV Airframe Projected Area, A_1 [m^2]	0.0599	0.224	11
Battery Projected Area, A_2 [m^2]	0.0037	0.015	N/A
Payload Projected Area, A_3 [m^2]	0 to 0.0135	0 to 0.0929	N/A
UAV Drag Coefficient, c_{D_1}	1.49	1.49	0.098
Battery Drag Coefficient, c_{D_2}	1	1	N/A
Payload Drag Coefficient, c_{D_3}	2.2	2.2	N/A
Battery Energy Density, e_{batt} [Wh/kg]	150	150	150
Transfer Efficiency (from Battery to Propellers), η	0.7	0.7	0.7
Maximum Depth of Discharge of the Battery, DoD	0.8	0.8	0.8
Maximum Discharge Rate of the Battery, C_R	10	10	10
Avionics Power, P_A, [kW]	0.02	0.1	6

Table 1: Parameter values of each multicopter model.

2.2 Fuel Cell System

A benchmarking of fuel cells and hydrogen storage cylinders is conducted, selecting those that best fit each UAV (see Table 2 and Table 3). For fuel cells, the key criteria in the choosing procedure include, maximum power, weight, and efficiency, parameters directly related with power density and fuel consumption, $\dot{m}_{H_2}$ [g/h] [3] [22],

$$\dot{m}_{H_2} = \frac{n_{FC}P}{LHV\eta_{FC}}. \tag{1}$$

Here P is the required power [W] and LHV is the Lower Heating Value of the hydrogen (equal to 33.3 Wh/g). For the rest of variables, consult Table 2. η_{FC} is not always publicly disclosed by manufacturers, thus in cases where it is unknown, a typical value of 0.5 is assumed, according to [2].

Meanwhile, for cylinders, the main characteristics considered are weight and the maximum amount of hydrogen they can store, directly related with the energy density. If the mass of stored hydrogen is not provided by the manufacturer, it can be estimated based on the pressure and volume of the cylinder. According to [22], 21 g of H_2 can be stored per liter at 300 bar, increasing to 24 g at 350 bar. In this study, only hydrogen in gaseous state is considered, as storage in cryogenic liquid state, despite the fact that its percent by weight compared to the total mass of the tank is doubled, with current technologies it is not worthwhile [8]. This is because it is challenging to store, prone to leaks, difficult to handle and operate, and too expensive [1] [19].

In order to apply the equations to be shown in 2.4 and compare hydrogen fuel cells with batteries, $m_2 = n_{FC}m_{FC} + n_C m_C$, $A_2 = n_{FC}A_{FC} + n_C A_C$, $\eta = 0.9$ (the drivetrain efficiency of electronics and electric motors [14]), and c_{D_2} will be considered the same as in batteries due to lack of data.

2.3 Flight Mission

Although there is no consensus on a specific flight profile for UAM routes, based on the proposals of various publications, the general case may be summarized as it is explained in [6]: taxi on the vertiport, vertical takeoff,

Fuel Cell	UAV	Maximum Power [kW]	Number of Fuel Cells, n_{FC}	Fuel Cell Mass, m_{FC} [kg]	Fuel Cell Area, A_{FC} [m^2]	Fuel Cell Efficiency, η_{FC}
IE SOAR 800 [11]	Small	0.8	1	1.45	0.01599	0.5
IE SOAR 2.4 [10]	Medium	2.4	2	3.73*	0.0298	0.5
A-4000 [13]	Medium	4	1 or 2	7	0.0492	0.534
FCmove®-XD [4]	Large	120	1 or 2	250	0.444	0.5

Table 2: Fuel cell specifications.

Cylinder	UAV	Hydrogen Capacity, m_{H_2}, [g]	Number of Cylinders, n_C	Cylinder Mass + Hydrogen Regulator, m_C [kg]	Cylinder Area, A_C [m^2]	Fuel Utilization Factor, η_{H_2}
SL50*[22][11]	Small	17.4	1	0.92	0.0093	0.95
SL77* [22][11]	Small	26.7	1	1.14	0.01	0.95
CFRCYL-III-12L [23] [24]	Medium	288	1	3.8	0.1207	0.95
QT/110500 [8]	Large	1550	3 or 8	20.3	N/A	0.95

Table 3: Hydrogen cylinder specifications.

transition phase from vertical takeoff to horizontal flight, climbing flight, cruise, descent in horizontal flight, transition from horizontal flight configuration to vertical, hovering, vertical landing, and taxi on the vertiport. Then, each study adapts this profile to its particular case. Transition phases are omitted in the case of multicopters, as there is no need to change the flight configuration [6]. In [20], the descent from the cruise flight level to the ground is completely vertical, with an intermediate hover of 30 s to allow prior clearances for landing and to correct the position of the aircraft. In [15], a multicopter takeoffs and lands directly with a 45-degree angle, omitting vertical phases as well as taxiing. In [21], both taxiing and ascent/descent phases are omitted, conducting vertical takeoff and landing from ground level to cruise altitude and vice versa, with an intermediate hover of 30 s.

In this work, transition phases are omitted by considering multicopters only. In addition, taxiing, descent, and landing phases are not simulated, not because they do not exist, but because they are less demanding for the propulsion system, both in terms of time (energy) and power, hence they will not be limiting factors.

2.4   Flight Analysis

This section will present the equations applied to obtain the energy consumption and the power required in each maneuver. Additional details for these equations can be found in [16] and [18].

2.4.1   Hovering

Based on the principles of *momentum theory* developed for helicopters, the ideal power required to maintain a rotorcraft in hovering is

$$P_{i_0} = Tv_i \equiv Tv_h = \sqrt{\frac{m^3 g^3}{2\rho A}}, \tag{2}$$

where T is the thrust, which must be equal to the total weight of the multicopter, v_h is the induced velocity during hovering in the rotor plane of a steady, incompressible, inviscid, axisymmetric one-dimensional flow model, v_i is

the induced velocity in the rotor plane, ρ is the atmospheric density (henceforth, 1.225 kg/m^3), m is the total mass of the UAV i.e. $m = m_1 + m_2 + m_3$, g is the gravitational acceleration (henceforth, 9.807 m/s^3), and $A = n\pi R^2$. is the total disk area of the rotors, where n is the number of the rotors and R is their radius.

In rotor analysis, it is common to use dimensionless parameters to generalize aerodynamic performance. Therefore, the *rotor thrust coefficient* reads

$$C_T = \frac{T}{\rho A v_T^2}, \tag{3}$$

with $v_T = \sqrt{6mg/n\rho RNc\bar{c}_l}$ the *tip speed*, N the number of blades per rotor, c the blade chord length and $\bar{c}_l$ the blade lift coefficient . To neglect non-ideal effects, correction coefficients have to be included to obtain more realistic results. Among them, the tip loss factor and the profile drag standout. The first one models how lift rapidly decreases as the blade tip is approached, producing induced effects. A typical value is $\kappa = 1.15$, obtaining a corrected ideal power for hovering of

$$P_i = \kappa P_{i_0} = \kappa T v_i \equiv \kappa T v_h. \tag{4}$$

The second estimates the power consumed due to drag in blades. It can be approximated by the *blade element method* applied to rectangular blades (c_d can be assumed to be constant), obtaining

$$P_{profile} = \rho A v_T^3 \frac{\sigma c_d}{8}, \tag{5}$$

where $\sigma = \frac{BladeArea}{DiskArea} = \frac{Nc}{\pi R}$ is the *rotor solidity*. Now, it is possible to recalculate the rotor aerodynamic power requirements (P_{aero}) using

$$P_{aero} \equiv P_{hover} = (\kappa P_{i_0} + P_{profile}) = (P_i + P_{profile}), \tag{6}$$

reading in its dimensional form

$$C_P = \frac{P}{\rho A v_T^3} = \frac{\kappa C_T^{3/2}}{\sqrt{2}} + \frac{\sigma c_d}{8}. \tag{7}$$

2.4.2 Climbing in Steady Flight and Cruise

During climbing, rotors must produce lift and propulsive force, as the UAV not only needs to maintain a hover but also overcome the resistance force generated by the UAV moving through the air and gravity to ascend. For that purpose, multicopters must form an angle of attack (α) relative to the oncoming flow and a flight path angle for climbing (γ) (see Figure 1).
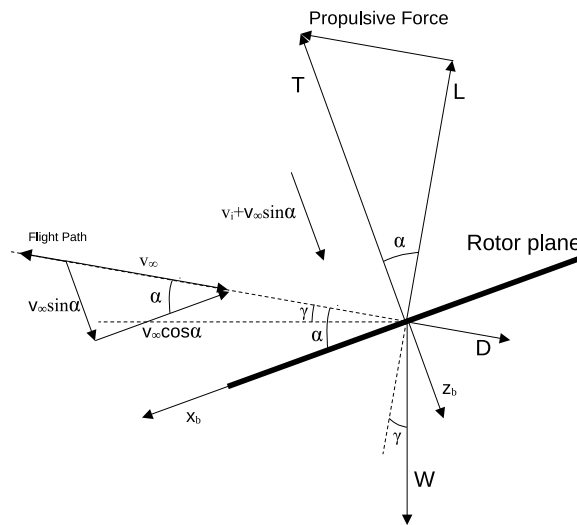
Figure 1: Inlet flow model and forces acting in a rotor during climbing in steady flight.

The relationship between these angles is

$$\tan(\alpha) = \frac{D + mg\sin(\gamma)}{mg\cos(\gamma)}, \tag{8}$$

where D is the drag force, dependent on the UAV airspeed V_∞, and the area and drag coeffficients of the UAV airframe ($A_3c_{D_3}$), batteries ($A_3c_{D_3}$) and payload ($A_3c_{D_3}$)

$$D = \frac{1}{2}\rho V_\infty^2 (A_1c_{D_1} + A_2c_{D_2} + A_3c_{D_3}). \tag{9}$$

To balance such force, a new power component $P_{parasite} = DV_\infty$ is required. On the other hand, in order to ascend, it is necessary to overcome the gravitational force with a power input of $P_{gravity} = mgV_\infty \sin(\gamma)$. Additionally, due to the forward flight, the flow does not penetrate perpendicular to the rotor, appearing an edgewise component of velocity ($V_\infty \cos(\alpha)$ in Figure 1). Thus, the axisymmetric condition is not longer true and the rotor operates in a more complex flow field, changing the induced and profile power equations, which can be rearranged as:

- Induced Power.

  From Figure 1, the resultant velocity at the rotor is

$$U = \sqrt{(V_\infty \cos\alpha)^2 + (V_\infty \sin\alpha + v_i)^2}, \tag{10}$$

  and the necessary thrust

$$T = \sqrt{m^2g^2 + D^2 + 2Dmg\sin(\gamma)}. \tag{11}$$

  In addition,

$$T = 2\rho AU v_i = 2\rho A v_i \sqrt{(V_\infty \cos\alpha)^2 + (V_\infty \sin\alpha + v_i)^2}. \tag{12}$$

  Thus, v_i can be computed iteratively from (12) and the induced power can be calculated as in (4).

- Profile Power. The forward flight will affect to $\bar{c}_l$ such as

$$\bar{c}_l = \frac{6C_T}{\sigma(1 + \frac{3\mu^2}{2})} = \frac{6C_T}{\sigma(1 + \frac{3V_\infty^2 \rho AC_T}{2T})}, \tag{13}$$

  where $\mu = V_\infty/v_T$ is the advance ratio. Moreover, the profile power is defined as

$$P_{profile} = \rho A v_T^3 \frac{\sigma c_d}{8}(1 + 3\mu^2). \tag{14}$$

  Then,

$$P_{aero} = P_{profile} + P_i + P_{gravity} + P_{parasite}. \tag{15}$$

Notice that during cruising, UAVs perform horizontal flights, which are a particular case of the climbing flight that occurs when the flight path angle is equal to zero ($\gamma = 0$), and then $P_{gravity} = 0$.

2.4.3 Vertical Flight

The formulation for this mode is similar to the hover case, but considering that the flow velocity at the rotor plane is $V_c + v_i$, being V_c the ascending velocity of the multicopter. The following equations relate hover flight with vertical flight:

$$\frac{v_i}{v_h} = -\frac{V_c}{2v_h} + \sqrt{\left(\frac{V_c}{2v_h}\right)^2 + 1}, \tag{16}$$

$$\frac{P_{aero}}{P_{hover}} = \frac{V_c}{v_h} + \frac{v_i}{v_h}. \tag{17}$$

2.4.4 Endurance and Range

The previous cases only had considered the aerodynamic power. Nevertheless, the drivetrain efficiency and the power consumption of the onboard avionics must be also included in the model, reading

$$P_{net} = (P_{aero})/\eta + P_A. \tag{18}$$

For batteries, the maximum power at which they can operate is $C_R m_2 e_{bat}$ [12], being C_R the maximum discharge rate of the batery and e_{bat} the battery energy efficiency. If this condition is satisfied, the endurance will be [16][29]:

$$t_e = \frac{m_2 e_{batt} DoD}{P_{net} f}, \tag{19}$$

where f is the factor to reserve energy in case of unusual conditions, considered with a constant value of 1.2 for all simulations and DoD is the maximum depth of discharge of the battery. Whereas for fuel cells, endurance is calculated as in [2],

$$t_e = \frac{m_{H_2} \eta_{H_2} n_C}{\dot{m}_{H_2}}. \tag{20}$$

Now, for both electric power systems, it is straightforward to determine the range $r = t_e V_\infty$.

3 Results and Analysis

Multiple simulations are conducted by modifying the mass and area of the payload (m_3 and A_3), and the speed of the multicopters. The mass starts at 0 kg (no payload) and is increased by a 0.1 kg step until reaching the maximum value of m_3 ($m_{3_{max}}$) for the medium and small UAVs, while for the large one, the increment is increased up to 1 kg. In case of the medium and small UAVs, the payload area is estimated according to the formulation proposed in (21), aiming to establish a relationship between the size and weight of the package, whereas in the large one this parameter does not compute because the payload is located inside the airframe. Finally, the dynamics of the UAVs begin with a static state (hover), and their forward speed is increased with a step of 0.1 m/s until reaching the power limit allowed according to each model. This process is performed for cruise, 45°climbing and vertical flight. Main results, organized by UAV model, are summarized in the data below, from Table 4 to Table 6. The last two columns of Table 6 consider an hybrid model, which will be explained in 3.1.

$$A_{3_i} = \left(\frac{i * step}{m_{3_{max}}}\right)^{2/3} A_{3_{max}} \quad \text{being} \quad i \in \mathbb{N}\left[0, \frac{m_{3_{max}}}{step}\right] \tag{21}$$

Notice that $\frac{m_{3_{max}}}{step}$ is always a natural number in all these simulations. Otherwise, the equation should be adapted.

Raw results suggest that both hovering and horizontal range and endurance are considerably improved (doubled and even tripled) by fuel cells, as long as the power is sufficient, whereas other more demanding maneuvers are worsen. In this regard, the case of the intermediate-sized UAV is particularly striking, where the payload must be significantly reduced, leading to a loss of operability and performance. Additionally, another drawback of this model is that the cruise flight speed, defined as the speed that maximizes range [20], is much lower than in the case of batteries. However, considering the power-to-weight ratio values, they are comparable to those of the other UAVs, even slightly better in some cases. Furthermore, analyzing only the battery values, the maximum flight time is 0.26 h, less than what is estimated for current battery-powered multicopters (0.33 to 0.83 h) [2].

Therefore, the issue may not lie in the type of propulsion but rather in the design parameters of the UAV themselves.Two parameters standout in the medium-sized UAV: the blade chord length (c) and the blade drag coefficient c_d, which are very high compared to the other aircraft. The first parameter is directly related with the rotor solidity, σ. In [18], it is explained that higher values of σ increment the viscous drag in rotors. Therefore, σ should be reduced minimizing the net blade area, but within cautious limits, as a very low value will lead to blade stall. Typical values of σ for helicopters are from 0.05 to 0.12 [18], which are similar to the values obtained in the small and large UAVs (0.157 and 0.055, respectively), but very distant from that of the medium-sized drone (0.59). This may explain why the c_d of the blade in the medium case (0.075) is much higher than in the others, where they are practically equal (0.012 and 0.015).

W/O = Without Payload. W/MP = With Maximum Payload (0.5 kg).

Term	Battery		IE SOAR 800 + SL50		IE SOAR 800 + SL77	
	W/O	W/MP	W/O	W/MP	W/O	W/MP
Maximum Power [kW]	1.5	1.5	0.8	0.8	0.8	0.8
Maximum Energy [kWh]	0.15	0.15	0.579	0.579	0.889	0.889
Maximum Range [km]	11.3	8.29	24.5	19.5	34.7	27.9
Maximum Endurance [h]	0.34	0.25	0.64	0.52	0.87	0.72
% Power Used for Max. Endurance	19.4	26	57.5	68.9	63.8	77.5
Maximum Hovering Endurance [h]	0.29	0.21	0.539	0.44	0.73	0.6
Optimal Cruise Speed [m/s]	11.6	11.7	13.6	13.5	14.2	13.9
Maximum Horizontal Speed [m/s]	24.2	21.5	17.3	14.8	16.7	13.9
Maximum Vertical Speed [m/s]	28	21.6	6.9	3.6	4.9	1.7
Maximum Climbing Speed [m/s]	20.4	17.4	10.2	6.8	8.6	4.3
Weight [kg]	2.07	2.57	3.44	3.94	3.65	4.15
Power-to-Weight Ratio [kW/kg]	0.72	0.58	0.23	0.2	0.219	0.19
Energy-to-Weight Ratio [kWh/kg]	0.07	0.05	0.16	0.14	0.24	0.21

Table 4: Performance of the Small-Sized UAV.

W/O = Without Payload. W/MP = With Maximum Payload (7 kg). W/3.3 = With 3.3 kg Payload. W/5.8 = With 5.8 kg Payload.

Term	Battery		2 x IE SOAR 2.4 + CFRCYL-III-12L			2 x A-4000 + CFRCYL-III-12L		
	W/O	W/MP	W/O	W/3.3	W/MP	W/O	W/5.8	W/MP
Maximum Power [kW]	15	15	4.8	4.8	4.8	8	8	8
Maximum Energy [kWh]	1.5	1.5	9.5	9.5	9.5	9.5	9.5	9.5
Maximum Range [km]	11.1	7	30.4	22.3	N/A	23.5	16	14
Maximum Endurance [h]	0.26	0.15	0.72	0.56	N/A	0.49	0.35	0.31
% Power Used for Max. Endurance	25.4	42.7	69	88.6	N/A	65	90	100
Maximum Hovering Endurance [h]	0.23	0.14	0.64	0.5	N/A	0.439	0.32	N/A
Optimal Cruise Speed [m/s]	16.5	17.1	16	12.4	N/A	18.1	13.9	12.2
Maximum Horizontal Speed [m/s]	31.3	25	16.8	12.4	N/A	20.1	13.9	12.2
Maximum Vertical Speed [m/s]	24.9	14.9	4.1	0.1	N/A	6	0.1	N/A
Maximum Climbing Speed [m/s]	26	18.8	9.0	0.7	N/A	11.7	0.5	N/A
Weight [kg]	17	24	18.26	21.56	25.26	24.8	28.7	31.8
Power-to-Weight Ratio [kW/kg]	0.88	0.63	0.26	0.22	0.19	0.32	0.27	0.25
Energy-to-Weight Ratio [kWh/kg]	0.08	0.06	0.52	0.44	0.37	0.38	0.33	0.29

Table 5: Performance of the Medium-Sized UAV.

In order to try to redesign the blades to obtain a more optimized model, two parameters related with the hovering efficiency are introduced: the figure of merit (FM) and the power loading (PL). FM allows for comparing the actual power required for hovering (P_{hover}, see (6)) with the ideal power (P_{i_0}, see (2)), leading to

$$FM = \frac{P_{i_0}}{P_{hover}} = \frac{P_{i_0}}{\kappa P_{i_0} + P_{profile}} = \frac{\frac{C_T^{3/2}}{\sqrt{2}}}{\frac{\kappa C_T^{3/2}}{\sqrt{2}} + \frac{\sigma c_d}{8}}. \tag{22}$$

On the other hand, PL is the thrust per unit of power that rotors can generate (T/P). A high power loading means that rotors will be more efficient, as less power is needed to maintain the aircraft in hovering. From equations 3 and 7,

$$\frac{P}{T} = \frac{v_T C_P}{C_T} = \frac{v_T}{C_T} \left(\frac{\kappa C_T^{3/2}}{\sqrt{2}} + \frac{\sigma c_d}{8} \right). \tag{23}$$

Thus, the maximum power loading can be obtained differentiating 23 with respect to C_T and equaling to zero.

W/O = Without Payload. W/MP = With Maximum Payload (200 kg).
*Compressible flow effects at the blade tip and forward speed are not taken into account.

Term	Battery		1 x FCmove®-XD + 3 x QT/110500		2 x FCmove®-XD + 8 x QT/110500		Hybrid System (1 x FC + 3 x QT + 30 kg Bat.)	
	W/O	W/MP	W/O	W/MP	W/O	W/MP	W/O	W/MP
Maximum Power [kW]	450	450	120	120	240	240	120 (165)	120 (165)
Maximum Energy [kWh]	45	45	154.8	154.8	412.9	412.9	154.8 (159.3)	154.8 (159.3)
Maximum Range [km]	58.6	46.5	189.0	150.2	174.7	148.5	182.2	146.6
Maximum Endurance [h]	0.43	0.30	1.38	0.98	1.05	0.82	1.3	0.94
% Power Used for Max. Endurance	15.4	21.8	49.5	65.6	40.7	51.9	47.2	68.6
Maximum Hovering Endurance [h]	0.26	0.18	0.84	N/A	0.63	0.49	0.79	(0.14)
Optimal Cruise Speed [m/s]	52.5	58.9	54.2	64.6	64.0	69.4	54.3	60.6
Maximum Horizontal Speed [m/s]*	125.4	121.1	73.8	64.6	96.4	90.0	72.5 (84.9)	63.0 (77.6)
Maximum Vertical Speed [m/s]	23.5	17	3.5	N/A	6.1	2.3	2.7 (6.5)	(1.9)
Maximum Climbing Speed [m/s]	51.2	38.7	10.2	N/A	16.5	8.0	8.6 (16.6)	(6.8)
Weight [kg]	700	900	710.9	910.9	1062.4	1262.4	740.9	940.9
Power-to-Weight Ratio [kW/kg]	0.64	0.5	0.16	0.13	0.22	0.19	0.16 (0.22)	0.12 (0.17)
Energy-to-Weight Ratio [kWh/kg]	0.06	0.05	0.21	0.16	0.38	0.32	0.20 (0.21)	0.16 (0.16)

Table 6: Performance of the Large-Sized UAV.

Substituting the result into 22, FM must be equal to $\frac{2}{3\kappa} \approx 0.58$. If $C_T = \frac{\bar{c}_l \sigma}{6}$ [16], then $c_d \approx 0.056\sqrt{\sigma}$. Thus, for a $c_d = 0.015$, σ will be equal to 0.072, which fits already in the typical range. Now, from the rotor solidity equation shown in 2.4.1, maintaining constant the number of blades, $c \approx 0.075R$.

Considering a radius of 0.25 m, a blade length chord of 0.0189 m is obtained, and the performance of the UAV can be recalculated. Table 7 summarizes the new results, demonstrating a notably improvement, with fuel cells surpassing the values of the batteries by 2 to more than 6 times in terms of horizontal flight and hovering. It is remarkable that now only a single A-4000 fuel cell is needed, allowing for an increase in range and flight time as the fuel consumption is halved and the weight is reduced. On the contrary, if more power is desired, it is possible to combine two fuel cells and lift the maximum payload with ease. The last two columns of Table 7 consider an hybrid model, which will be explained in 3.1.

W/O = Without Payload. W/MP = With Maximum Payload (7 kg).

Term	Battery		1 x A-4000 + CFRCYL-III-12L		2 x A-4000 + CFRCYL-III-12L		Hybrid System (1 x A-4000 + CFRCYL + 1.5 kg Bat.)	
	W/O	W/MP	W/O	W/MP	W/O	W/MP	W/O	W/MP
Maximum Power [kW]	15	15	4	4	8	8	4 (6.25)	4 (6.25)
Maximum Energy [kWh]	1.5	1.5	9.5	9.5	9.5	9.5	9.5 (9.72)	9.5 (9.72)
Maximum Range [km]	19.44	11.54	111.1	69.0	38.78	26.31	102.9	64.6
Maximum Endurance [h]	0.45	0.26	2.74	1.65	0.84	0.57	2.44	1.52
% Power Used for Max. Endurance	27.4	46.7	46.7	77.4	37.9	55.9	52.4	84.2
Maximum Hovering Endurance [h]	0.35	0.21	2.18	1.35	0.67	0.46	1.94	(1.0)
Optimal Cruise Speed [m/s]	15.1	15.3	14.4	14.9	16.3	16.4	14.9	14.0
Maximum Horizontal Speed [m/s]	35.0	28.8	20.4	14.9	25.6	21.0	19.9 (24.0)	14.0 (19.1)
Maximum Vertical Speed [m/s]	35.1	23.3	7.8	0.8	13.2	7.1	6.2 (12.5)	(5.6)
Maximum Climbing Speed [m/s]	29.4	22.7	12.4	3.0	17.5	11.8	11.0 (16.5)	(10.1)
Weight [kg]	17	24	17.8	24.8	24.8	31.8	19.3	26.3
Power-to-Weight Ratio [kW/kg]	0.88	0.62	0.22	0.16	0.32	0.25	0.2 (0.32)	0.15 (0.23)
Energy-to-Weight Ratio [kWh/kg]	0.08	0.06	0.53	0.38	0.38	0.29	0.49 (0.5)	0.36 (0.36)

Table 7: Results of the Improved Medium UAV.

3.1 Hybridization

Hybridization aims to obtain both the advantages of fuel cells (higher energy density) and the benefits provided by batteries (higher power density) in a single system. Consequently, throughout the course of the mission, UAVs will fly thanks to the fuel cells, and when facing more demanding operations such as increased speed or vertical and climbing flights, they can obtain extra power for a few minutes from batteries. However, as a trade-off, hybrid systems increase weight and size, which can result in a loss of payload capacity or overall performance.

In the last two columns on the right of Table 6 and Table 7, the characteristics for a hybrid system of the large-sized UAV, consisting of 1 FCmove®-XD, 3 cylinders QT/110500, and 30 kg of batteries, and the medium-sized UAV, consisting of 1 FC A-4000, 1 cylinder CFRCYL-III-12L, and 1.5 kg of batteries are presented. The values in parentheses are those obtained when the batteries are active. Batteries provide sufficient power during demanding maneuvers, ensuring a minimum autonomy of 4 minutes per charge. Meanwhile, fuel cells enable the UAVs to longer missions. Additionally, with the surplus energy of fuel cells, batteries could be recharged during the flight, incurring minimal energy costs for the fuel cells (it is not included in the simulation, but a total battery charge would represent less than the 3 % of the stored energy both in the large-sized and medium-sized UAVs). Thus, the weight of both UAVs is significantly reduced compared to incorporating a second fuel cell while maintaining similar performance (see Figure 2(a) and 2(b)), hydrogen consumption is less than half, which means that range and endurance is incremented (see Figure 2(c) and 2(d)), and overall costs are much lower, as the estimated price per kWh for batteries ranges from 110 $/kWh to 129 $/kWh, while for fuel cells, it rises to 239 $/kWh [26].

(a)

(b)

(c)

(d)
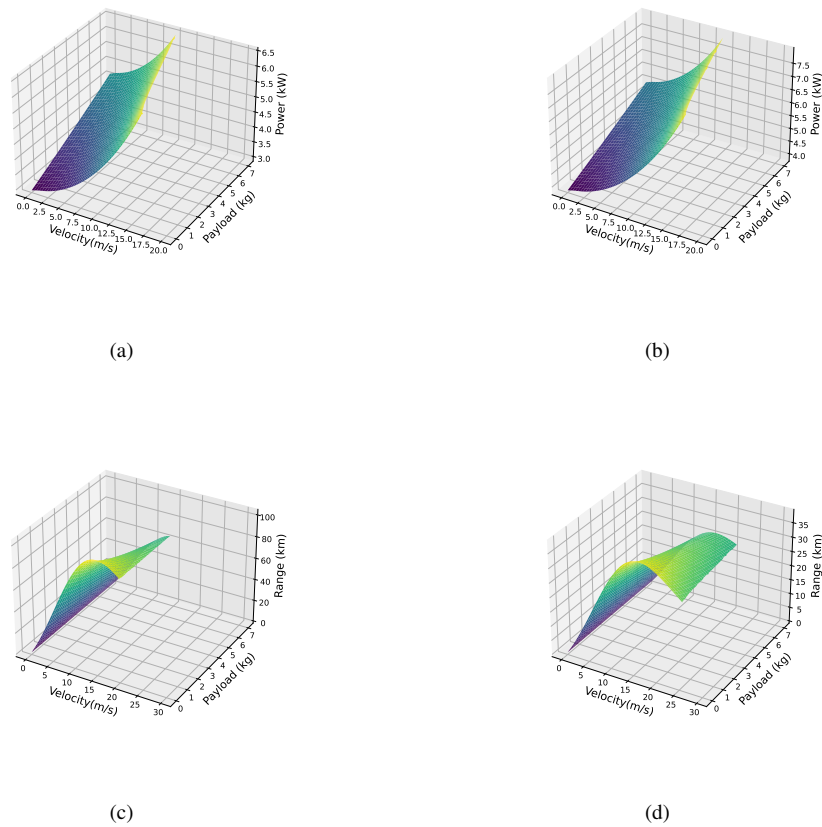
Figure 2: Example of the performance of the medium-sized modified UAV. a) Range with the Hybrid System. b) Range with 2 FC A-4000. c) 45-degree climbing speed with the hybrid system. d) 45-degree climbing speed with 2 FC A-4000.

Regarding the small UAV, hybridization lacks justification, as the fuel cell alone can perform all types of operations. Additionally, the total weight of the UAV with the introduction of the fuel cell and cylinder is more than 1.5 times the weight of the original UAV, and the additional battery would further increase the total weight of the quadcopter, making it inoperable. In contrast, for the medium and large-sized UAVs, weight remains practically constant.

4 Conclusions

It is expected that multicopters will play a fundamental role in UAM. However, one of their main challenges is the limited flight time due to the low energy density of batteries. This study explores the possibility of using fuel cells

as an alternative. Simulations are conducted on three UAVs of very different sizes and weights during the most demanding and critical flight phases, leading to the following conclusions:

- Horizontal range, and both hovering and horizontal endurance are considerably improved by fuel cells (from 2 to 6 times).

- In the case of fuel cells, the payload capacity can be affected if the UAV design is not optimized, while for batteries, this factor is not as crucial due to their higher power density.

- The optimal flight speed does not change significantly, although it generally increases slightly in the case of hydrogen cells and hybrid systems, potentially reducing the flight time.

- In vetical and 45-degree climbing flights, speeds are worsen with the use of fuel cells, reaching levels that may be too low or even making it impossible to lift the UAV due to lack of power. For medium and large multicopters, this issue can be addressed with a hybrid system by incorporating batteries that provide additional power during peak demand moments. In the case of small-sized UAVs, hydrogen fuel cells must have sufficient power to lift them as the increment of weight is too high to accommodate additional components.

- Hybridization allows for cost, weight and consumption reduction in medium and large-sized UAVs, as each system can be designed to operate in its optimal form.

- Batteries exhibit higher power-to-weight ratio (from 2.5 to 4 times), while energy-to-weight ratio is significantly improved with hydrogen fuel cells (from 3.5 to 6.5 times in medium and large UAVs and 2 to 4.5 in small-UAVs, since small cylinders have a lower weight percentage of hydrogen.)

Additionally, further research should be conducted, including more realistic environments involving meteorology, obstacles, control, and dynamics of UAVs, as well as real tests comparing different propulsion systems. However, based on the simulations and the results obtained, fuel cells appear to be a viable alternative to batteries.

ACKNOWLEDGMENT

References

[1] J. Apeland, D. Pavlou, and T. Hemmingsen. State-of-Technology and Barriers for Adoption of Fuel Cell Powered Multirotor Drones. In *2020 International Conference on Unmanned Aircraft Systems (ICUAS)*, pages 1359–1367. IEEE, 9 2020.

[2] Jørgen Apeland, Dimitrios Pavlou, and Tor Hemmingsen. Suitability Analysis of Implementing a Fuel Cell on a Multirotor Drone. *Journal of Aerospace Technology and Management*, 8 2020.

[3] Zayd Aslam, Adrian Felix, Christos Kalyvas, and Mahmoud Chizari. Design of a Fuel Cell/Battery Hybrid Power System for a Micro Vehicle: Sizing Design and Hydrogen Storage Evaluation. *Vehicles*, 5:1570–1585, 11 2023.

[4] Ballard. FCmove^{TM}-XD.

[5] Arthur Brown and Wesley L. Harris. Vehicle Design and Optimization Model for Urban Air Mobility. *Journal of Aircraft*, 57:1003–1013, 11 2020.

[6] Robert Brühl, Hartmut Fricke, and Michael Schultz. Air taxi flight performance modeling and application. In *Fourteenth USA/Europe Air Traffic Management Research and Development Seminar (ATM2021)*, 2021.

[7] Yong Sik Chang and Hyun Jung Lee. Optimal delivery routing with wider drone-delivery areas along a shorter truck-route. *Expert Systems with Applications*, 104:307–317, 8 2018.

[8] Anubhav Datta and Wayne Johnson. Requirements for a Hydrogen Powered All-Electric Manned Helicopter. In *12th AIAA Aviation Technology, Integration, and Operations (ATIO). Conference and 14th AIAA/ISSMO Multidisciplinary Analysis and Optimization Conference.* American Institute of Aeronautics and Astronautics, 9 2012.

[9] European Union Aviation Safety Agency (EASA). Study on the societal acceptance of Urban Air Mobility in Europe, 2021.

[10] Intelligent Energy. IE-SOAR 2.4 fuel cells for drones.

[11] Intelligent Energy. IE-SOAR 800 hydrogen fuel cells for UAVs.

[12] ELB Energy Group. Battery C Rating Explanation And Calculation.

[13] H^3 Dynamics. AEROSTAK A-4000.

[14] Nasser Hashemnia and Behzad Asaei. Comparative study of using different electric motors in the electric vehicles. In *2008 18th International Conference on Electrical Machines*, pages 1–5. IEEE, 9 2008.

[15] Thomas Kirschstein. Comparison of energy demands of drone-based and ground-based parcel delivery services. *Transportation Research Part D: Transport and Environment*, 78:102209, 1 2020.

[16] Jack W. Langelaan, Sven Schmitz, Jose Palacios, and Ralph D. Lorenz. Energetics of rotary-wing exploration of Titan. In *2017 IEEE Aerospace Conference*, pages 1–11. IEEE, 3 2017.

[17] Tao Lei, Zhou Yang, Zicun Lin, and Xiaobin Zhang. State of art on energy management strategy for hybrid-powered unmanned aerial vehicle. *Chinese Journal of Aeronautics*, 32:1488–1503, 6 2019.

[18] Gordon Leishman. *Introduction to Aerospace Flight Vehicles.* Embry-Riddle Aeronautical University, 2022.

[19] P. Millet. *Hydrogen storage in hydride-forming materials*, pages 368–409. Elsevier, 2014.

[20] Michael D. Patterson, Kevin R. Antcliff, and Lee W. Kohlman. A Proposed Approach to Studying Urban Air Mobility Missions Including an Initial Exploration of Mission Requirements. In *AHS International 74th Annual Forum and Technology Display*, 2018.

[21] Michael Shamiyeh, Raoul Rothfeld, and Mirko Hornung. A Performance Benchmark of Recent Personal Air Vehicle Concepts. In *31st Congress of the International Council of the Aeronautical Sciences, ICAS*, 09 2018.

[22] IE SOAR. Guide to Cylinder Options for UAV Applications. Cylinder options for UAVs.

[23] SPECTRONIK. Carbon Fiber Cylinders.

[24] SPECTRONIK. Miniature gas pressure regulator.

[25] Joshuah K. Stolaroff, Constantine Samaras, Emma R. O'Neill, Alia Lubers, Alexandra S. Mitchell, and Daniel Ceperley. Energy use and life cycle greenhouse gas emissions of drones for commercial package delivery. *Nature Communications*, 9:409, 2 2018.

[26] Technology Trends team at the APC. Battery and fuel cell future cost comparison, 2023.

[27] Ashleigh Townsend, Immanuel N. Jiya, Christiaan Martinson, Dmitri Bessarabov, and Rupert Gouws. A comprehensive review of energy sources for unmanned aerial vehicles, their shortfalls and opportunities for improvements. *Heliyon*, 6:e05285, 11 2020.

[28] Meiling Yue, Hugo Lambert, Elodie Pahon, Robin Roche, Samir Jemei, and Daniel Hissel. Hydrogen energy systems: A critical review of technologies, applications, trends and challenges. *Renewable and Sustainable Energy Reviews*, 146:111180, 8 2021.

[29] Juan Zhang, James F. Campbell, Donald C. Sweeney II, and Andrea C. Hupman. Energy consumption models for delivery drones: A comparison and assessment. *Transportation Research Part D: Transport and Environment*, 90:102668, 1 2021.